Electric Field Switching of the Magnetic Anisotropy of a Ferromagnetic Layer Exchange Coupled to the Multiferroic Compound $BiFeO_3$

D. Lebeugle,[1] A. Mougin,[1] M. Viret,[2,*] D. Colson,[2] and L. Ranno[3]

[1]*Laboratoire de Physique des Solides, Université Paris-Sud, CNRS UMR 8502, 91405 Orsay Cedex, France*

[2]*Service de Physique de l'Etat Condensé, CEA Saclay, DSM/IRAMIS/SPEC, URA CNRS 2464, 91191 Gif sur Yvette, France*

[3]*Institut Néel, CNRS and Université Joseph Fourier, 38042 Grenoble, France*

(Received 4 September 2009; published 14 December 2009)

We report here that a Permalloy layer deposited on top of a multiferroic $BiFeO_3$ single crystal acquires an easy magnetic direction along the propagation vector of the cycloidal arrangement of antiferromagnetic moments in $BiFeO_3$. This anisotropy originates from a direct magnetic coupling with the canted spins forming the cycloid. Moreover, we show that an electric field-induced change of electric polarization is able to toggle the direction of anisotropy in the ferromagnet through the magnetoelectric effect, which links the antiferromagnetic spins to the local polarization in $BiFeO_3$.

DOI: 10.1103/PhysRevLett.103.257601 PACS numbers: 77.80.Fm, 75.30.Gw, 75.70.−i, 77.84.−s

The bifunctionality of the multiferroic materials [1,2], which present simultaneous ferroelectric (FE) and magnetic orders is a property of great interest for designing potential devices, particularly in spintronics and magnetic data storage. Indeed, controlling the magnetization of a ferromagnetic (FM) layer with electric fields via the interaction called ''magnetoelectric coupling'' may lead to the conception of electrically addressable magnetic memories. Unfortunately, very few materials possess simultaneously an electrical polarization and a net magnetization. Instead, most multiferroics are antiferromagnetic (AF) ferroelectrics where the two orders are coupled, which is the case in the only material (and its substituted derivatives) showing multiferroicity at room temperature: $BiFeO_3$ (BFO). This compound is noncentrosymmetric with a rhombohedric distortion ($a = 3.96$ Å and $\alpha = 89.4°$, space group $R3c$) and it orders electrically below $T_C = 1143$ K [3] and antiferromagnetically (G type) below $T_N = 643$ K. Magnetoelectric coupling induces a local spin canting of the Fe^{3+} moments which order forming a long-range cycloid leading to zero total magnetization [4]. The antiferromagnetic and polarization vectors are linked and the magnetic moments have to rotate in a plane containing the direction of polarization, $\vec{P}_S$, (along the [111] direction) and the cycloidal propagation vector [4]. Because of the rhombohedral symmetry, there are three equivalent directions for the cycloid in a domain of polarization along [111], which are $\vec{q}_1$ [1-10], $\vec{q}_2$ [10-1], and $\vec{q}_3$ [0-11]. It is also known that in thin film form BFO changes drastically because the cycloid becomes unstable and a small global magnetization is recovered [5].

In order to electrically control a net magnetic moment, one can deposit a FM layer on top of BFO and use the exchange coupling at the interface between antiferromagnetic and FM bilayers [6,7]. This magnetic coupling has provided, since its discovery [8], an important challenge to the understanding of interfaces between magnetic materials. Its most visible experimental signature is a shift, or ''bias,'' of magnetization hysteresis loops, which depends on magnetic history (via, e.g., field cooling through the AF ordering temperature). In most cases, the FM coercivity is also enhanced and easy and hard directions can be induced. Overwhelming literature has emerged in which various mechanisms for this exchange bias and related effects have been proposed, debated, and tested (see, e.g., [9]). It has also been shown that an exchange coupling exists in BFO/CoFeB bilayers [10,11] and preliminary experiments have even revealed the possibility to locally control ferromagnetism with an electric field using $BiFeO_3$ as the multiferroic layer [7]. It is not clear where the bias fields come from but they may originate from the weak canting (due to the magnetoelectric effect), of the order of 0.02°, between neighboring spins leading to a net moment in the BFO films. In the bulk, this canting is much greater, around 1.6°, but it orders in a cycloid leading to zero net magnetization. Therefore, locally, a stronger exchange coupling could be expected with bulk BFO, albeit with the absence of long-range ferromagnetic order.

Using a flux technique, we have synthesized high quality BFO single crystals [12]. They are millimetric, highly resistive, and also often electrically and magnetically single domain [4,13]. The polarization has to lie along the long diagonals of the pseudocubic unit cell, leading to 8 possible ferroelectric domains and 2 possible directions for the domain walls: {110} and {100}. Since the crystals form platelets along the (001) plane, the electric field can only be applied at an angle of 54.7° from the polarization directions. Thus, after poling, the crystals can never be fully saturated again as 4 domain types with different in-plane projections are equally stable. The majority of the crystals used as substrates for deposition of Permalloy (Py) were ferroelectrically single domain or contained another small minority domain. After a slight 2 min etching, thin layers (5 to 20 nm) of Py ($Ni_{78}Fe_{22}$)

were deposited in a 200 Oe magnetic field of various directions and then capped with a 3 nm layer of Au. Over ten samples have been measured which show a similar behavior. Most of the results reported in this Letter are from a single $BiFeO_3$ crystal on which the full set of our measurements has been carried out including crystallographic orientation by four-circle x-ray diffraction, magneto-optical Kerr effect (MOKE) measurements, *E*-field poling, magneto-optical imaging in applied magnetic and electric fields.

The Py layers deposited on BFO all present two nonequivalent in-plane magnetic directions: an easy and a hard axes oriented at 90° from each other. The angular evolution of the remanent magnetization and the field at which an irreversible jump is observed in the hysteresis loops are plotted in a polar curve on Fig. 1. Because the switching is obtained when the component of fields along the easy axis exceeds the anisotropy field, its maximum (reaching around 15 mT) corresponds exactly to the hard axis direction, where the remanent magnetization is also zero. Conversely, at 90°, the remanence is 100% and the switching field is lowest, indicating the easy direction. Interestingly, the exchange bias, if any, is always below 0.2 mT. This could be due to the full compensation of the magnetization in the [100] type planes imposed by the cycloid. However, it is known that a bias can arise due to roughness induced uncompensated spins, whose number is often inversely proportional to the size of the AF domains. Alternatively, loose spins could be located in the domain walls themselves. In both cases, a large density of domain walls would be needed to generate a bias. This is consistent with the existence of bias in thin films [6,7] where domains are small and its absence in crystals, which are almost single domain.

Importantly, in all the samples measured, the easy axis is found to be linked to the crystallographic axes of BFO, irrelevantly of the presence and direction of the magnetic field during deposition. For the sample of Fig. 1 the easy axis is along the [010] direction and the hard axis along [100]. At first sight, this result is surprising because these main cubic directions correspond neither to a projection of the polarization (i.e., the direction of strain), nor to a specific direction for the projection of the local moments. The only magnetic quantity having the right projection is the cycloid propagation vector. We believe that this can be understood considering the exchange coupling with the cycloidal arrangement of the magnetic moments. The local interfacial exchange energy can generally be written in the form $E_{ex} = J_{ex}\vec{S}_F(\vec{S}_{AF1} + \vec{S}_{AF2})$ where the indices 1 and 2 refer to the two AF sublattices. For a fully compensated AF, this energy averages to zero, but for $BiFeO_3$, it amounts to $E_{ex} = 1/2J_{ex}\vec{S}_F\vec{S}_{cant}$ where $\vec{S}_{cant}$ is the local spin canting from the Fe^{3+} moments describing the cycloid, which thus tends to imprint its shape into the ferromagnet. However, because the cycloid periods projected on the (100) plane (62 nm for that along $\vec{q}_1$ and 87 nm for those along $\vec{q}_2$ and $\vec{q}_3$) are on a length scale comparable to the exchange length (around 15 nm in Permalloy), the ferromagnet is not likely to adopt a cycloidal arrangement. Instead, the exchange coupling should induce a wriggling of the ferromagnetic magnetization along the underlying cycloid (see Fig. 2). We argue here that this wriggle is

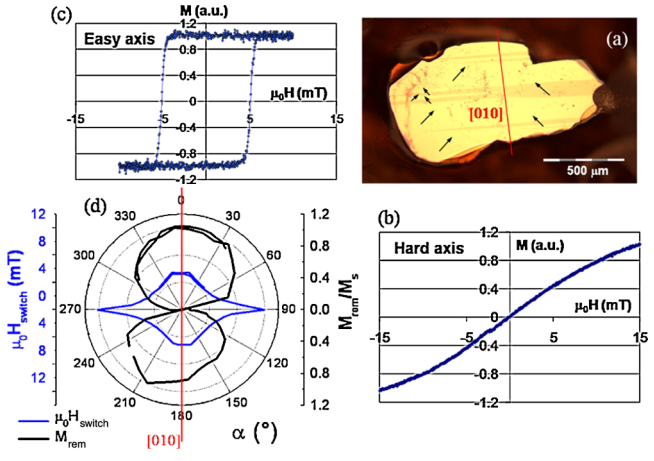

FIG. 1 (color online). (a) Polarized light image of a single crystal of $BiFeO_3$ whose long direction is along [100]. The contrast between bright and dark domains comes from the birefringence of the ferroelectric crystal. In the virgin state a few long minority domains can be seen with a common polarization direction accounting to about 10% of the total area. (b, c) MOKE hysteresis loops measured on the 10 nm thick Py layer deposited on the BFO crystal: an easy and a hard axes appear along, respectively, the [010] and [100] directions, as can be seen in the polar curve of the switching field and the remanent magnetization (d).

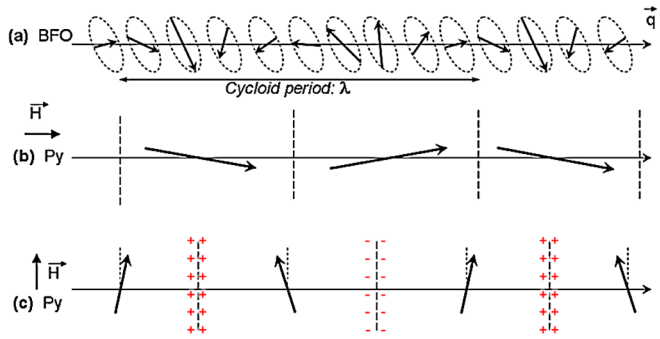

FIG. 2 (color online). (a) Schematics of the projection on the interfacial plane of the cycloidal spin arrangement in bulk BFO with propagation vector $\vec{q}$. (b,c) the Py magnetization is assumed to ripple following the component of the exchange field transverse to the FM magnetization, along the cycloid projection (the wriggling angle is largely overestimated for a better visibility). The state in (c) where the magnetization is globally perpendicular to $\vec{q}$ gives the highest demagnetization energy because the building of (virtual) magnetic charges at the domain borders is maximum, whereas it is negligible in (b).

responsible for the easy axis measured in the Py/BFO systems. Indeed, exchange energy and interfacial coupling with the cycloid do not depend on the global direction of magnetization while the demagnetizing energy is minimum when $M \parallel \vec{q}$ and maximum when $M \perp \vec{q}$ (see Fig. 2). Hence, an easy axis appears along the cycloid propagation vector. It is possible to estimate the angle of the wriggling magnetization needed to explain the measured anisotropy field of about 15 mT by considering the cost in demagnetizing energy when $M \perp \vec{q}$. In that case, the dipolar fields can be calculated when one simplifies the configuration to magnetic ellipsoidal domains at some small angle to one another (see Fig. 2). The anisotropy field, which has to overcome the demagnetizing field, is then given by $H_{\mathrm{an}} = \frac{4t}{\lambda} \mu_0 M \sin(\theta)$ where λ is the ripple period, t the ferromagnet thickness, M the magnetization, and θ the angle of the magnetization wriggle. To induce the observed anisotropy of 15 mT, one gets for θ a value close to 1.5°. The resulting exchange field is several times larger than that reported for BFO in thin film form [10], as can be expected from the larger local canting in the crystals.

In order to make a useful device with this phenomenon, one would need to address the magnetization of the ferromagnetic layer with an electric field. This is conceivable since when $\vec{P}$ changes, the antiferromagnetic vector in BFO toggles so that the Fe spins remain in the plane containing $\vec{P}$ and the cycloid propagation vector. Thus, the exchange induced easy axis should change. In order to check this, we have applied a 25 kV/cm electric field on the crystal of Fig. 1 that leads to a multidomain state consisting of a mosaic of ferroelectric domains with domain walls at angles of 45° and 180° between each other, as shown in Fig. 3. MOKE hysteresis loops were then measured as a function of the angle between the applied field H and BFO [100] through an aperture of 300 × 150 microns positioned in a region of the crystal where a mosaic of ferroelectric domains separated by domain walls along the [110] and [1-10] directions appeared after application of the electric field. Two contributions with two different sets of coercivities are visible in the hysteresis cycles (as seen in Fig. 3). Thus, the change in polarization has generated another domain of magnetic coupling in the Py. We have extracted, from the hysteresis loops at each angle, the coercivity (switching field) and remanence of this new domain by subtracting a contribution proportional to that measured in the initial polarization region. The polar curve shows that the easy and hard axes of this second domain are at 90° from those obtained before applying the electric field. As in the original virgin configuration, no net exchange bias is visible in this multidomain state.

In order to get additional information regarding the topological configuration of the electric and magnetic domains, we have imaged in real time the ferroelectric and ferromagnetic configurations during application of both

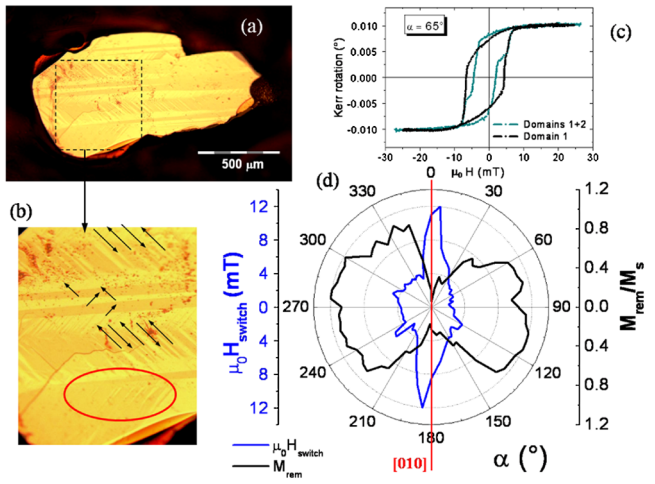

FIG. 3 (color online). (a) Ferroelectric image of the crystal after application of a 25 kV/cm electric field. (b) Shows a zoomed area where the arrows represent the in-plane projection of $\vec{P}$ and the red ellipse is a schematic of the laser spot for the MOKE measurements. (c) Typical hysteresis cycle obtained when $\vec{H}$ makes a 65° angle with the [100] direction. Two contributions are visible including one with the same coercive fields as the initial virgin state measurement (black curve). The second contribution, which appeared after application of the electric field, can be extracted by subtraction. (d) Polar curve of the angular dependence of the remanent magnetization and the switching field for the new contribution.

the electric and magnetic fields (Fig. 4). The imaging is carried out using a polarizing microscope in reflectivity mode in a configuration close to the 90°-crossed polarizer vs analyzer. Because the Py layer is thin (between 5 and 20 nm), a reasonable amount of light is transmitted through the metal and reflected back by the BFO. Thus, both information concerning the magnetic state of the Py and the ferroelectric state of the BFO are contained in the polarization rotation of the reflected light. However, because of the low thickness of our Py films and the small rotation angles induced by the Kerr effect, it is hard to extract the magnetic information from the overwhelming signal coming from the ferroelectric domains and it is essential to proceed by subtraction of a background image.

In order to check if it is possible to directly address the Py magnetization via the electric field, we have poled the sample while imaging the ferromagnetic domains. We find a clear modification of the magnetic easy axes in the Py following a pattern linked to the topology of ferroelectric domains. This is obviously related to the magnetoelectric effect in the BFO whereby a change of polarization is able to toggle the direction of the antiferromagnetic vector of the BFO [4]. Figure 4 compares images with electric and magnetic contrast at different stages of the repeated poling process. After the first poling to 25 kV/cm (and then back to zero electric field), a first set of images (FE1 and MAG1) show perfect correspondence between ferroelectric and

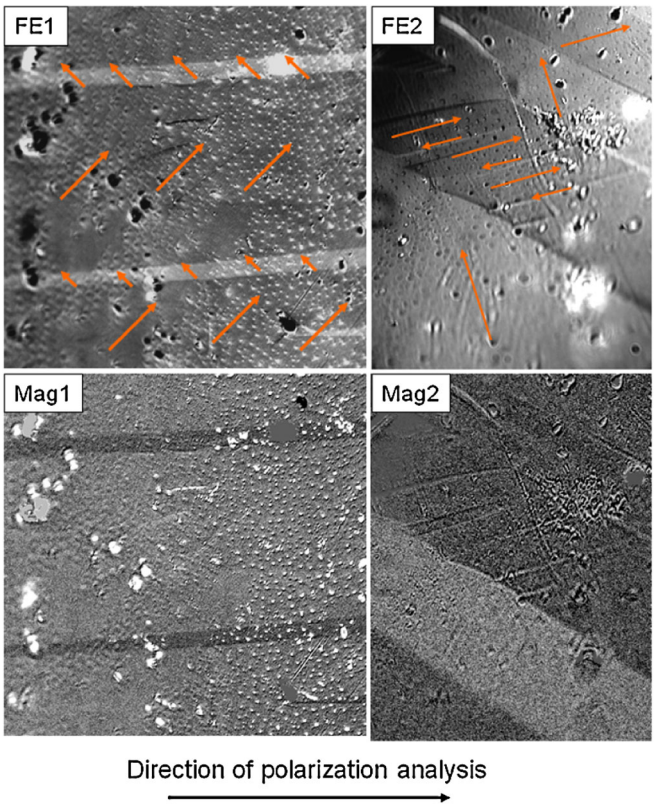

FIG. 4 (color online). Comparison of ferroelectric (FE) and magnetic (MAG) images in two areas (1 and 2) of the crystal. After the first poling (set 1), there is a one to one correspondence between FE and magnetization domains. (FE2) and (MAG2) are similar images obtained after the electric field was swept 5 times. The white magnetic domain, which systematically reverses first, has a border corresponding to a ferroelectric domain wall but another one in the middle of a large polarization domain.

magnetic domains (whose contrast can be inverted by reversing the applied magnetic field). The second set of images (FE2 and MAG2) were taken while sweeping the magnetic field after the sample was poled electrically 5 times. Systematically, the magnetic regions in the Py showing cooperative reversal did not exactly match the polarization domains of the BFO underneath. This can be seen in Fig. 4 where the bottom majority domain in MAG2 has a clear border inside the large BFO ferroelectric domain visible in FE2. This is consistent with a magnetic coupling depending on the topology of the cycloids in BFO, which are not rigidly attached to the polarization, as for any given $\vec{P}$ three possible cycloids can exist. Moreover, it is possible to have a common propagation vector [4] where for instance, $\vec{q}_3$ is common to $\vec{P}_1[111]$ and $\vec{P}_2[-111]$ domains (oriented at 70.5° to each other). Thus, the topology of the exchange coupling does not have to correspond exactly to that of the ferroelectric domains. Figure 4 suggests that the toggling of the antiferromagnetic vectors during poling can generate several cycloids in any polarization domain. Conversely, some cycloids also have a common propagation vector between neighboring FE domains, as evidenced by the cooperative behavior of the Py region covering the chevron shaped ferroelectric domains visible in FE2.

To conclude, our measurements show that the exchange coupling between Py layers and BFO crystals result in a uniaxial anisotropy following the cycloids made by the Fe^{3+} moments in the BFO. An applied electric field reorients the polarization and thus modifies the easy magnetic axes in the Py. Unfortunately, although the exchange coupling is locally stronger than that with BFO films, it is not able to directly reorient a macroscopic Py magnetization. Since the cycloids in BFO are the key to the coupling, a better control of their direction via the magnetoelectric interaction with the polarization is essential if one wants to electrically address a magnetization with an electric field. This might be possible in a nanostructure with a complete control of the polarization reversal process.

We thank X. Le Goff for the x-ray measurements, S. Pizzini for lending us the Kerr imaging setup, and M. Bibes and A. Barthelemy for enlightening discussions. We acknowledge support by the Agence Nationale de la Recherche, project ''MELOIC'' ANR-08-P196-36.

*michel.viret@cea.fr

[1] N. Spaldin and M. Fiebig, Science **309**, 391 (2005).
[2] W. Eerenstein, N. Mathur, and J. Scott, Nature (London) **442**, 759 (2006).
[3] J. Moreau, C. Michel, R. Gerson, and W. James, J. Phys. Chem. Solids **32**, 1315 (1971).
[4] D. Lebeugle *et al.*, Phys. Rev. Lett. **100**, 227602 (2008).
[5] H. Bea *et al.*, Appl. Phys. Lett. **87**, 072508 (2005); H. Bea *et al.*, Philos. Mag. Lett. **87**, 165 (2007).
[6] T. Zhao *et al.*, Nature Mater. **5**, 823 (2006); J. Dho *et al.*, Adv. Mater. **18**, 1445 (2006).
[7] Y. H. Chu *et al.*, Nature Mater. **7**, 678 (2008).
[8] W. Meiklejohn and C. Bean, Phys. Rev. **102**, 1413 (1956).
[9] J. Nogués and I. Schuller, J. Magn. Magn. Mater. **192**, 203 (1999).
[10] H. Béa *et al.*, Phys. Rev. Lett. **100**, 017204 (2008).
[11] L. W. Martin *et al.*, Nano Lett. **8**, 2050 (2008).
[12] D. Lebeugle *et al.*, Phys. Rev. B **76**, 024116 (2007).
[13] D. Lebeugle, D. Colson, A. Forget, and M. Viret, Appl. Phys. Lett. **91**, 022907 (2007).